The published version of the paper "Filippo Ubertini, Gabriele Comanducci, Nicola Cavalagli, Anna Laura Pisello, Annibale Luigi Materazzi, Franco Cotana, Environmental effects on natural frequencies of the San Pietro bell tower in Perugia, Italy, and their removal for structural performance assessment, Mechanical Systems and Signal Processing, Volume 82, 2017, Pages 307-322, ISSN 0888-3270" is available at: https://doi.org/10.1016/j.ymssp.2016.05.025.

Environmental effects on natural frequencies of the San Pietro bell tower in Perugia, Italy, and their removal for structural performance assessment

Filippo Ubertini[a,d], Gabriele Comanducci[a], Nicola Cavalagli[a], Anna Laura Pisello[b,c], Annibale Luigi Materazzi[a], Franco Cotana[b]

[a] *Department of Civil and Environmental Engineering, University of Perugia, Via G. Duranti 93, 06125 Perugia, Italy*

[b] *CIRIAF Interuniversity Research Center on Pollution and Environment "M. Felli", University of Perugia, Via G. Duranti, 06125 Perugia, Italy*

[c] *Department of Engineering, University of Perugia, Via G. Duranti 1/A4, 06125 Perugia, Italy*

[d] *Corresponding author, phone: +39 075 585 3954; fax: +39 075 585 3897; e-mail: filippo.ubertini@unipg.it*

Abstract

Continuously identified natural frequencies of vibration can provide unique information for low-cost automated condition assessment of civil constructions and infrastructures. However, the effects of changes in environmental parameters, such as temperature and humidity, need to be effectively investigated and accurately removed from identified frequency data for an effective performance assessment. This task is particularly challenging in the case of historical constructions, that are typically massive and heterogeneous masonry structures characterized by complex variations of materials' properties with varying environmental parameters and by a differential heat conduction process where thermal capacity plays a major role.

While there is abundance of documented monitoring data highlighting correlations between environmental parameters and natural frequencies in the case of new structures, such as long-span bridges, similar studies for historical constructions are still missing, with only a few literature works occasionally reporting increments in natural frequencies with increasing temperature of construction materials due to the closure of internal micro-cracks in the mortar layers caused by thermal expansion.

In order to gain some knowledge on the effects of changes in temperature and humidity on the natural frequencies of slender masonry buildings, the paper focuses on the case study of an Italian monumental bell tower that has been monitored by the authors for more than nine months. Correlations between natural frequencies and environmental parameters are investigated in details and the predictive capabilities of linear statistical regressive models based on the use of several environmental continuous monitoring sensors are assessed. At the end, three basic mechanisms governing environmentally-induced changes in the dynamic behavior of the tower are identified and essential information is achieved on the optimal location and minimum number of environmental sensors that are necessary in a structural health monitoring perspective.

Keywords: structural health monitoring, environmental effects, cultural heritage preservation, historical constructions, weather conditions, continuous hygro-thermal monitoring, operational modal analysis.

---

1. Introduction

Extracting dynamic signatures from vibrating structures and inspecting their variations is becoming a popular engineering practice for automated structural performance assessment and early stage damage detection [1], whereby a structural damage can be in many cases detected as a modification in the global dynamic behavior of the structure [2, 3]. This automated detection of small changes in structural performance, typically produced by earthquakes or by other types of dynamic loadings, allows a cost-effective management of maintenance and restoration interventions which is named condition-based maintenance as opposite to breakdown-based or periodic maintenance [4].

While traditionally applied to civil infrastructure [5], vibration-based structural health monitoring (SHM) techniques appear to be very promising for applications to slender historical and monumental structures, such as civic towers and bell towers [6]. This is due to their fully non-destructive character and the relatively inexpensive equipment that is necessary for testing (usually a small number of high sensitivity accelerometers and off-the-shelf devices for data acquisition, storage and analysis), resulting in historical and architectural respect conforming to international criteria and protocols on cultural heritage preservation. Despite all these advantages, only a few applications of continuous vibration-based SHM systems to cultural heritage constructions have been documented so far [7], whereby the majority of the authors have limited their attention to ambient vibration testing for complementing vulnerability assessment through calibration of finite element models: the interested reader could benefit of literature devoted to applications to historical bridges [8, 9, 10], monumental buildings [11, 12, 13, 6, 14] and historical towers [15, 16, 17, 18, 19, 20, 21]. A more widespread application of continuous SHM in the context of historical constructions is however expected in the near future, especially as it concerns civic and bell towers that typically exhibit higher amplitudes of vibration in comparison to low-rise buildings, thus being comparatively more suited for dynamic monitoring.

Natural frequencies of vibration have recently been rediscovered as very effective and convenient damage sensitive features for vibration-based SHM [22]. One main reason making natural frequencies so attractive is that reliable automated operational modal analysis (OMA) techniques have been developed in recent years [23, 24, 25], allowing an accurate estimation of natural frequencies from in-service response data, typically using a small number of off-the-shelf sensors and without requiring any manual intervention. Unfortunately, natural frequencies have the main drawback of being strongly affected by environmental conditions and above all key weather parameters, such as temperature and humidity [1] as well as, in the case of very slender structures, wind speed [26]. In order to cope with this issue, some authors have proposed to remove the part of variance in the data associated with changing environmental conditions through the use of proper statistical models, such as multiple data regressions [27] and principal component analysis (PCA) [28, 29, 30] and to detect anomalies in the structural behavior by means of statistical process control tools such as control charts [27, 31, 32]. While the mechanisms governing environmentally-induced variations of natural frequencies in modern structures have been mostly clarified, characterization and removal of the key environmental effects from continuously identified natural frequencies of historical masonry constructions is still an open problem, due to the lack of documented permanent monitoring campaigns in such kind of structures. In this context, some authors reported an increase in the natural frequencies of vibration of global modes of masonry towers with increasing outdoor dry bulb temperature due to thermal expansion in the masonry determining closing of micro-cracks in mortar layers [6, 7], but the knowledge in this field needs further investigation as addressed in this research work.

This paper presents an in-depth characterization of environmental effects on the natural frequencies of vibration of a monumental masonry bell tower, the San Pietro bell tower in Perugia, Italy, where the authors have recently installed a permanent vibration-based SHM system. The paper is organized as follows. Section 2 presents the case study historical tower and the multipurpose monitoring system. Section 3 investigates correlations among environmental parameters and among natural frequencies, as well as cross-correlations between natural frequencies and the monitored environmental parameters. Section 4 addresses the task of statistical estimation of natural frequencies from independent environmental measurements by investigating, in particular, the role played by the number of environmental monitoring sensors, their optimal placement and the length of the training period necessary for identifying the statistical models. Finally, Section 5 concludes the paper.

2. Continuous structural health monitoring of a monumental masonry bell tower

2.1. The bell tower

The case study considered in this paper is the bell tower of the Benedictine Abbey of San Pietro in Perugia, Italy, Figure 1. This monumental masonry tower, erected for the first time in the 13th century, can be considered as one of the major monuments of the City, owing to its unique architectural character and to its location on top of a hill from where it dominates the civic skyline.

With its total height of 61.45 m, the tower can be roughly subdivided in four main parts. The lowest section, termed basement, has a cone shape and reaches the height of about 8 m. The portion of the tower erected over the basement and reaching the height of 26 m is termed shaft and has a dodecagonal cross section. Both basement and shaft are made of hollow masonry with an internal core made of heterogeneous material. The total width of the walls of the basement ranges from 3.2 m on the base to about 2 m on the top. The external surfaces of such walls are made of regular calcareous stone blocks with some brick local replacements, while internal surfaces are made of less regular stone masonry. The four bells are located in the belfry that has an hexagonal cross-section and reaches the height of 41 m. The belfry is architecturally characterized by large Gothic openings presenting external frames and columns made of a mixed travertine-calcareous stone masonry with some brick replacements. The internal surface of the belfry is instead entirely made of brick masonry. Above the belfry, the tower is completed by the cusp that has the shape of a pyramid with hexagonal cross-section and is made of a mixed travertine-calcareous stone masonry with an external cover in brick masonry.

The bell tower as it appears today is the result of various structural and architectural modifications occurred through the centuries. The most invasive intervention was made in the 14th century when the tower was fully demolished and rebuilt as a defensive building. The final design, in Florentine Gothic style, was probably developed by Bernardo Rossellino in the 15th century. Other, more limited modifications to the structure showed to be necessary in order to repair damages caused by lightnings. In 1932, the vault at the base of the belfry was partially demolished in order to install the metallic structure that still supports the four bells. This intervention was probably motivated by the necessity to better distribute the dynamic loads that the swinging bells exerted on the structure. In 2002, the tower was repaired in order to fix the damages caused by the strong earthquake that occurred in Umbria and Marche central Italian regions in 1997. This intervention mostly affected the belfry and the cusp where damages were concentrated and consisted of grout injections at the base of the columns of the belfry, installation of fiber rings on the cusp, to withstand the lateral thrust at the top of the belfry, and application of longitudinal fiber strings along the inner parts of the columns to prevent bending deformations [33].

Fig. 1 reports a photo evidence of the tower and a solid CAD model of the structure highlighting its main geometrical characteristics.

2.2. Monitoring hardware

With the purpose of monitoring the structural integrity of the bell tower and of promptly detecting damages caused by low-return period earthquakes, a vibration-based SHM system has been installed by the authors at the end of 2014. The system comprises three high sensitivity accelerometers permanently installed at the base of the cusp and various environmental monitoring sensors and proper data acquisition hardware. Monitoring data are locally recorded and sent, through the Internet, to the Laboratory of Structural Dynamics of University of Perugia, where they are processed in a dedicated server for the purpose of modal tracking and SHM using a MatLab code [34] developed by the authors for the purpose, and to the laboratories of CIRIAF Interuniversity Research Centre on Pollution and Environment "Mauro Felli" for the purpose of monitoring of weather and other environmental conditions.

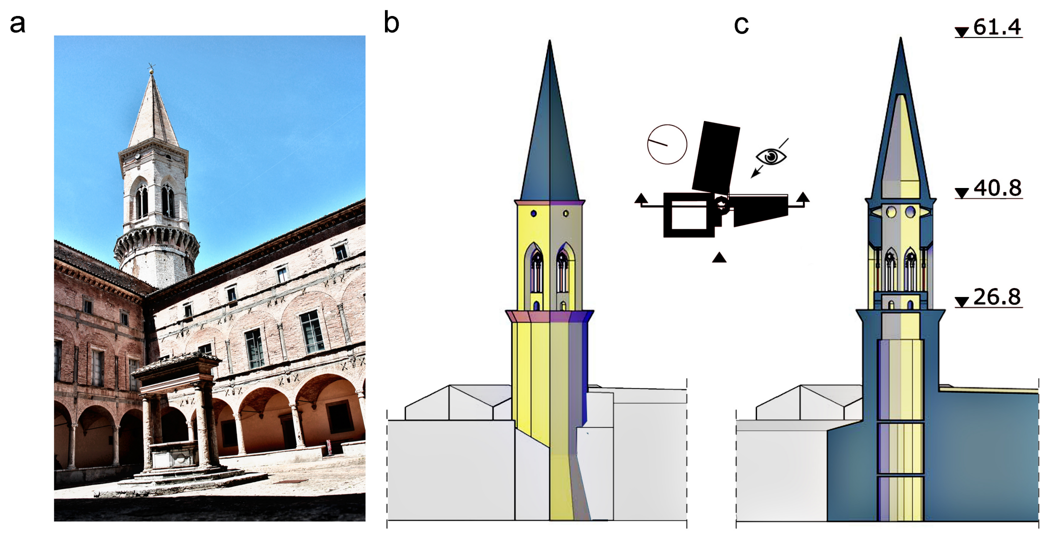

Figure 1: The bell tower of the Basilica of San Pietro (dimensions in m): photography from inner cloister (a); front view (b) and sectional view (c) from solid CAD model.

Accelerometers installed on site are uni-axial sensors model PCB 393B12 with 10 V/g sensitivity. The sensors' layout, shown in Figure 2, allows to observe bending modes in the two orthogonal directions denoted as x and y, as well as torsional modes.

With the purpose of achieving a spatially dense representation of the environmental conditions of the tower, eight temperature sensors (six dry bulb temperature sensors and two surface temperature sensors) and two humidity sensors have been installed since March 2015 with the layout shown in Figure 2. In this way, SHM and environmental monitoring are combined, which stimulates the development of integrated structural-thermal-energy monitoring systems for historic buildings. Environmental sensors are Tinytag from Gemini Data Loggers, typically used in building physics applications [35, 36, 37] and representing robust environmental monitoring solutions for field application in difficult accessibility locations such as the case study of this work. Table 1 summarizes the main information about temperature measurements, numbered from T_1 to T_8, and humidity measurements, denoted as ϕ_1 and ϕ_2.

Data from accelerometers are acquired through a multi-channel system, carrier model cDAQ-9188 with NI 9234 data acquisition modules (24-bit res-

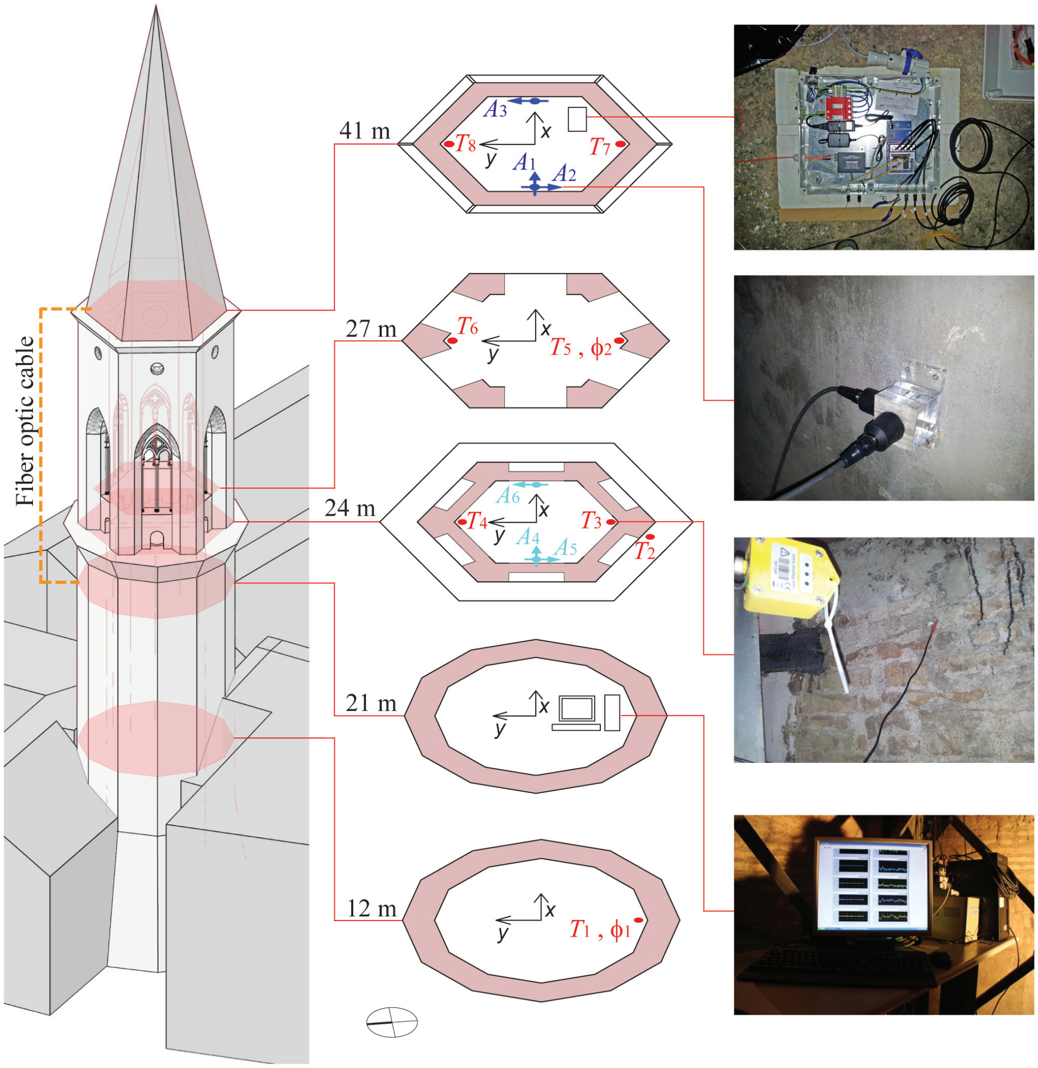

Figure 2: Sketch of the monitoring system with sensors positions and photo evidence of sensors on site and of data acquisition hardware (A, T and ϕ denote acceleration, temperature and humidity sensors, respectively). Acceleration sensors A_1, A_2 and A_3 are used for permanent monitoring purposes, while sensors A_4, A_5 and A_6 are only used in AVT.

olution, 102 dB dynamic range and anti-aliasing filters). Data from environmental sensors are acquired every 30 minutes and contemporary registered within indipendent dataloggers connected to each sensor.

Sensor no.	Variable name	Measurement type	Location	Height	Orientation
1	T_1	Air temperature	Shaft indoor	12 m	S
2	T_2	Surface temperature	Shaft outdoor	24 m	S
3	T_3	Surface temperature	Shaft indoor	24 m	S
4	T_4	Air temperature	Shaft indoor	24 m	N
5	T_5	Air temperature	Belfry outdoor	27 m	S
6	T_6	Air temperature	Belfry outdoor	27 m	N
7	T_7	Air temperature	Cusp indoor	41 m	S
8	T_8	Air temperature	Cusp indoor	41 m	N
9	ϕ_1	Air humidity	Shaft indoor	12 m	S
10	ϕ_2	Air humidity	Belfry outdoor	27 m	S

Table 1: Environmental monitoring sensors installed on the bell tower.

After the first months of monitoring, the system showed to be prone to overvoltage from the power line and to currents induced in wired connections by lightnings that quite often hit the tower during the year. In order to avoid consequent damaging to the monitoring hardware, the system has been occasionally shut down between December 2014 and August 2015, while protective countermeasures have been undertaken since August 2015. In order to avoid induced currents, accelerometers are connected to the data acquisition system using short cables, deployed in horizontal directions, orthogonal to the direction of the lightning rods. The use of short cables also reduces noise in the signals. The data acquisition system is located at the base of the cusp and placed within a box that contains a protective system against overvoltage. Electrical disconnection between sensors and masonry is also achieved by screwing the accelerometers to Plexiglas blocks rigidly connected to the structure (see Figure 2). A dedicated computer is placed in an accessible location below the belfry and it is used for data storage and for data transmission through the Internet. This computer is connected to the data acquisition system located inside the cusp using a 30 m long vertical fiber optic network cable that does not transmit induced currents. The monitoring system, including the protective system against lightnings, is depicted in Figure 2.

2.3. Continuous modal identification technique

Damage detection of the bell tower is based on the continuous identification of its natural frequencies and on the inspection of their variations associated with local changes in stiffness. Vibration data are recorded at

1600 Hz, down-sampled to 40 Hz and stored in separate files of 30 recording minutes for the purpose of modal identification.

Output only modal identification is carried out using 30-minutes long time history acceleration data by means of a fully automated data-driven Stochastic Subspace Identification (SSI-data) technique developed by the authors in a previous study [25]. It is worth noting that the duration of the signals contained in each monitoring file is fairly longer than what is classically suggested in the literature (e.g. [38]) for an accurate modal identification, that is, a duration larger than about 1000-2000 times the fundamental structural period.

SSI-data establishes a mathematical model of the monitored structure, based on output-only information, in the form of a linear-time-invariant system under unknown excitation:

$$\begin{aligned} \mathbf{x}(k+1) &= \mathbf{A}\mathbf{x}(k) + \mathbf{w}(k) \\ \mathbf{y}(k) &= \mathbf{C}\mathbf{x}(k) + \mathbf{v}(k) \end{aligned} \tag{1}$$

where k is the generic time step and $\mathbf{x} \in \mathbb{R}^n$ is the state vector, n being the order of the identified model. In eq. (1), $\mathbf{A} \in \mathbb{R}^{n \times n}$ is the system matrix from which modal information is retrieved, $\mathbf{w} \in \mathbb{R}^n$ is the unknown external input, modeled as a white noise vector process, $\mathbf{y} \in \mathbb{R}^l$ is the vector containing the l output measurements, $\mathbf{C} \in \mathbb{R}^{l \times n}$ is the corresponding output matrix and $\mathbf{v} \in \mathbb{R}^l$ is a white noise vector process representing the noise content of the measurements. For the details on the theory of SSI-data, the interested reader is referred to Ref. [39].

In the adopted automated identification procedure, the data-driven SSI canonical variate analysis is performed for different values of the order of the model in Eq. (1) and of the number of output block rows adopted to construct the block Hankel matrix of the data [39]. Then, spurious noise modes are eliminated on the basis of similarity checks between estimated modal parameters and clustering of remaining modes is carried out. Finally, mean values of modal parameters estimates with 95% confidence intervals are extracted from each cluster of modes.

In the present application, the order of the model is varied from 40 to 60 with step increments of 2 and the number of output block rows is varied from 140 to 200 with step increments of 10. Relative tolerances used for noise modes elimination are: 0.01 for frequencies, 0.03 for modal damping ratios and 0.01 for modal assurance criterion. Finally, a relative tolerance of 0.03 is used for clustering analysis as threshold in a similarity check comprising both frequencies and eigenvectors. The interested reader is referred to Ref. [25] for specific details on the identification procedure.

2.4. Environmental effects removal and health assessment methodology

Environmental effects can be removed from identified natural frequency data using statistical techniques [27, 28, 29, 30]. In this paper, multiple linear regressive (MLR) filters are adopted for this purpose, where linear correlations between a set of r dependent variables (natural frequencies) and a set of p independent variables (environmental parameters), called predictors, are exploited. In the present case, modal frequencies are stored in an observation matrix, $\mathbf{Y}$, and an estimate, $\hat{\mathbf{Y}}$, of such a matrix is obtained as

$$\hat{\mathbf{Y}} = \boldsymbol{\beta}^T \mathbf{Z}^T \tag{2}$$

where matrix $\mathbf{Z} \in \mathbb{R}^{N \times p+1}$ contains a first column of ones and p columns containing N values of the p selected environmental parameters, while matrix $\boldsymbol{\beta} \in \mathbb{R}^{p+1 \times r}$ contains constant terms in the first row and coefficients that weight the contribution of each environmental parameter in the remaining p rows.

The residual error matrix, $\mathbf{E}$, between identified and predicted natural frequencies is thus given by

$$\mathbf{E} = \mathbf{Y} - \boldsymbol{\beta}^T \mathbf{Z}^T \tag{3}$$

which represents the prediction error of the statistical model. The coefficients of the statistical model contained in matrix $\boldsymbol{\beta}$ are estimated in a least square sense by minimizing the norm of $\mathbf{E}$ in a reference training period.

Under the assumption that the MLR model is able to reproduce the part of variance in frequency estimates that is associated with changes in environmental conditions, quantities contained in the residual error matrix, $\mathbf{E} \in \mathbb{R}^{r \times N}$, during the monitoring period are unaffected by environmental parameters and are therefore used for structural health assessment.

A damage condition can be identified as an anomaly in the data contained in matrix $\mathbf{E}$, under the assumption that damage induces a change in their distribution. Such anomalies can be detected by the use of control charts based on properly defined statistical distances: a damage condition is identified as an outlier in the distribution of the statistical distance. A popular choice, for instance, is the use of the T^2-statistic, which is defined as

Mode number	Frequency [Hz]	Damping ratio [%]	Mode Type
1	1.449	1.0	Fx1
2	1.518	1.0	Fy1
3	4.342	1.6	T1
4	4.575	1.1	Fx2
5	4.889	2.3	Fy2
6	7.245	5.1	Fx3
7	7.263	2.7	Fy3

Table 2: Identified modal parameters of the bell tower during the AVT.

$$T^2 = s \cdot (\overline{\mathbf{E}} - \overline{\overline{\mathbf{E}}})^T \cdot \mathbf{\Sigma}^{-1} \cdot (\overline{\mathbf{E}} - \overline{\overline{\mathbf{E}}}) \tag{4}$$

where s is an integer parameter, referred to as *group averaging size*, $\overline{\mathbf{E}}$ is the mean of the residuals in the subgroup of the last s observations, while $\overline{\overline{\mathbf{E}}}$ and $\mathbf{\Sigma}$ are the mean values and the covariance matrix of the residuals, respectively. Both $\overline{\overline{\mathbf{E}}}$ and $\mathbf{\Sigma}$ are statistically estimated in the same training period used for estimating matrix $\boldsymbol{\beta}$ in Eq. (3).

3. Analysis of hygrothermal effects on natural frequencies

3.1. Frequency tracking

For the purpose of determining baseline modal parameters of the bell tower, an ambient vibration test (AVT) was carried out on February 16th 2015, with the main excitation provided by wind loading. Six high sensitivity piezoelectric uni-axial accelerometers of the same type of those used for monitoring (cfr. Section 2.2) were installed on the bell tower. Measurement channels are numbered from 1 to 6 in Figure 2. In particular, three accelerometers were located at the base of the cusp and three at the base of the belfry, thus instrumenting both the available floors within the tower.

Data were acquired using the same hardware adopted in the monitoring system and modal parameters were extracted from 30-minutes long AVT data using the SSI-data procedure described in Section 2.3. Identified natural frequencies, damping ratios and mode shape types are summarized in Table 2. Identified mode shapes are also shown in Fig. 3. Lateral modes are denoted as Fx and Fy, where x and y are the reference axes shown in Figure 2. The third mode is a torsional one and is denoted as T1.

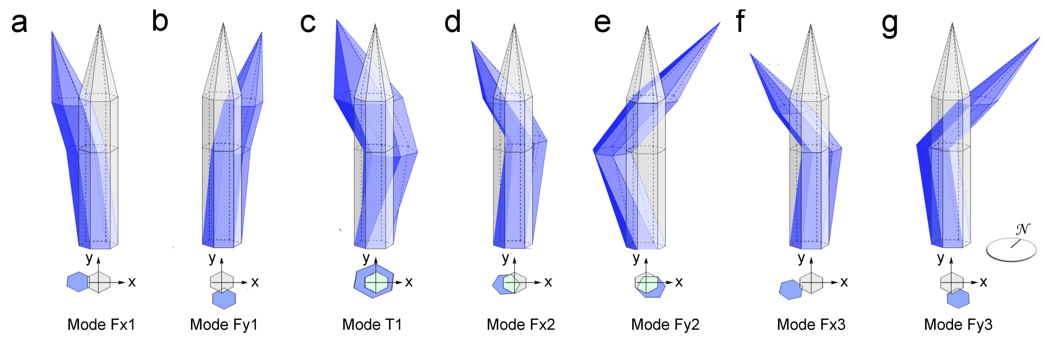

Figure 3: Identified mode shapes of the bell tower during the AVT.

The vibration monitoring system has started to continuously acquire acceleration data on December 9th 2014. Since then, time histories of identified modal parameters are available with a sampling time of 30 minutes, with occasional interruptions when it was necessary to shut down the system in order to prevent possible damages caused by lightnings hitting the tower during storms (cfr. Section 2.2).

Due to the low levels of vibration of the tower in operational conditions, some modes are only rarely identified. In particular, modal tracking was only possible for five modes: the first two bending modes, Fx1 and Fx2, the first torsional mode, T1, and the second and third bending modes in the y direction, Fy2 and Fy3, respectively. Fig. 4 shows identified modal frequencies versus time, where daily fluctuations are clearly apparent and some seasonal trends are also visible for some modes. As discussed later on, both daily fluctuations and seasonal trends showed to be essentially related to temperature variations, while the sharp increase in the frequency of mode Fy3 observed during the earliest days of 2015 was associated to freezing conditions.

3.2. Correlation analysis

Table 3 summarizes the correlation coefficients between environmental data during the monitoring period. The time history plots of the same environmental data are depicted in Fig. 5. These results show an overall large degree of correlation between temperature data recorded by different sensors, with some temperature measurements that are almost perfectly correlated. In particular, as also shown in Figure 5, temperatures $T_3 - T_4$, $T_5 - T_6$ and

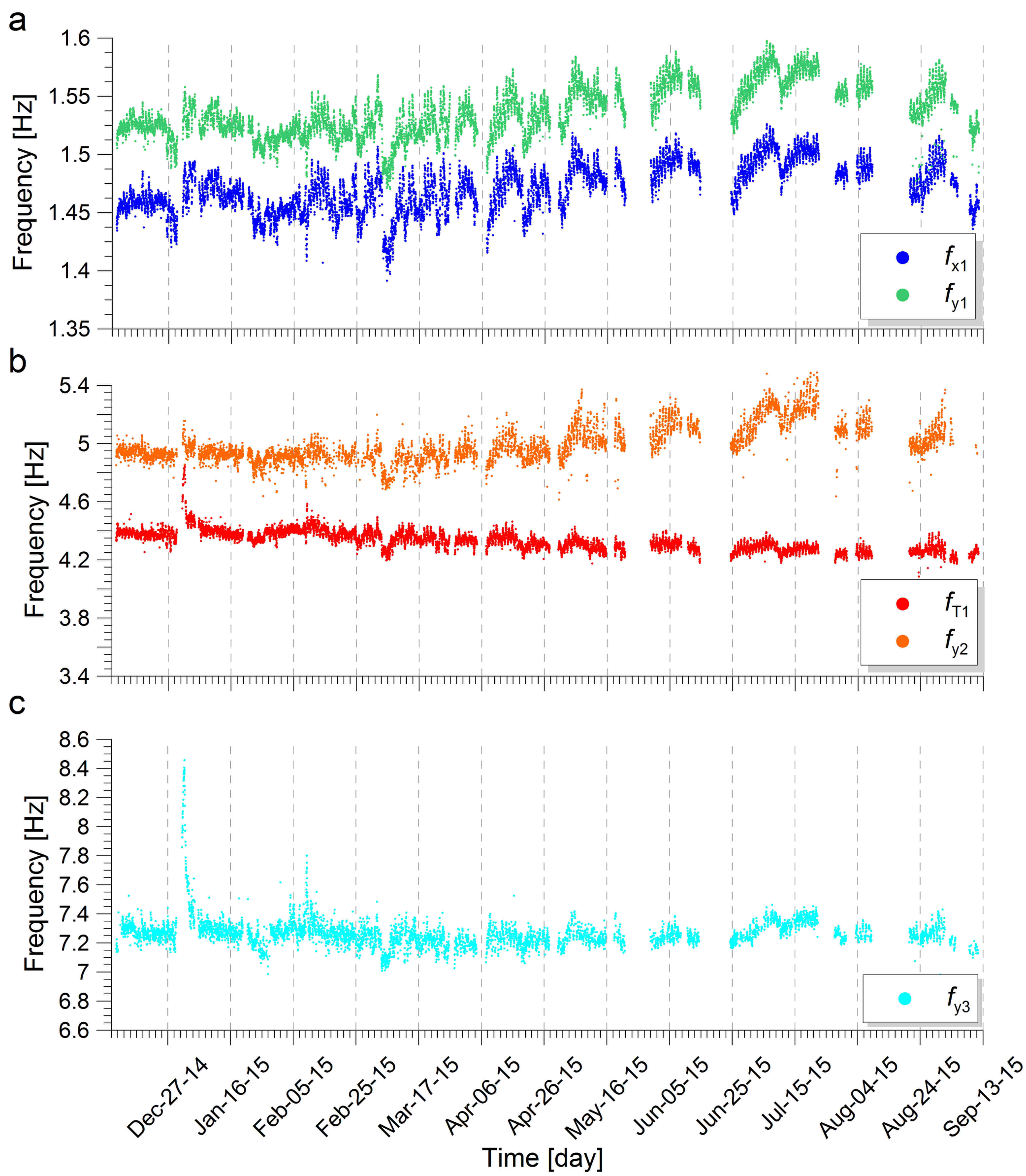

Figure 4: Identified natural frequencies of the bell tower versus time: frequencies of modes Fx1 and Fx2 (a); frequencies of modes T and Fy2 (b); frequency of mode Fy3 (c).

$T_7 - T_8$ are almost coincident, which explains their correlation coefficients being close to unit values.

In general, weaker correlations are observed between outdoor and indoor

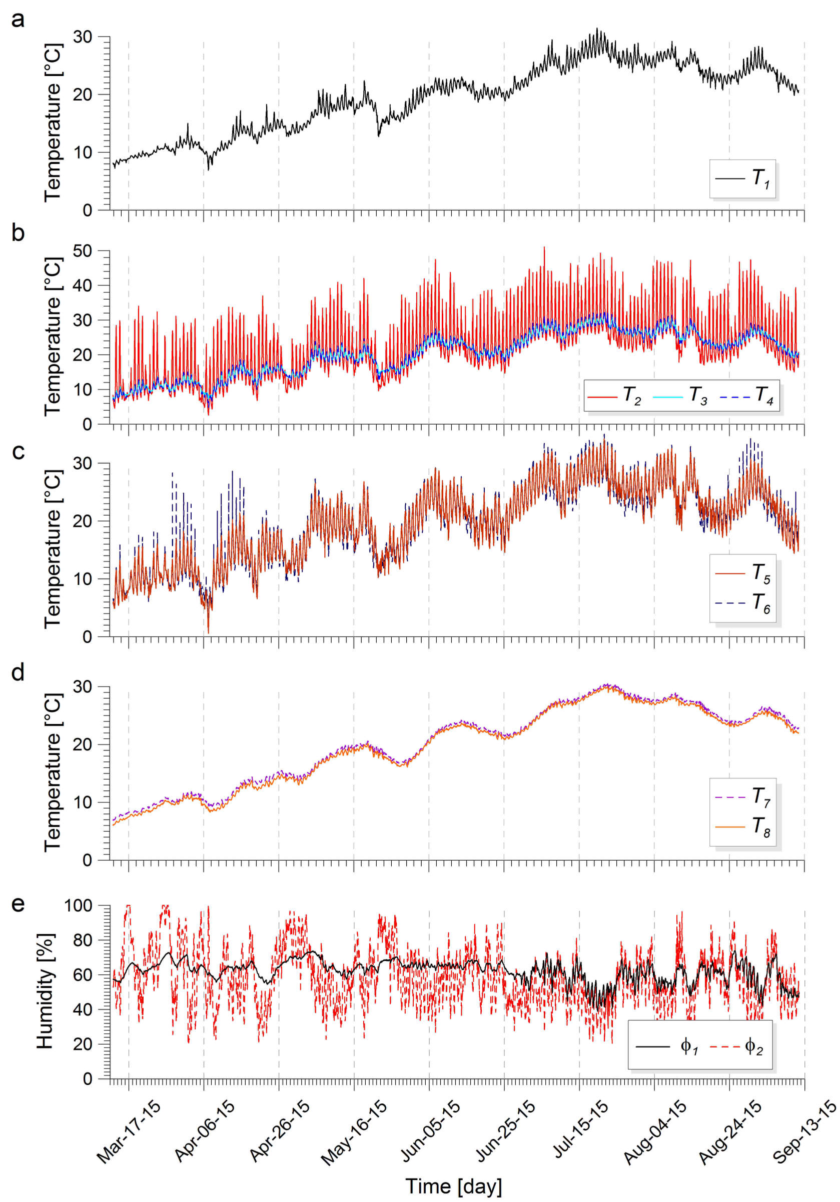

Figure 5: Time history plots of temperature and humidity measurements: T_1 (a); T_2, T_3 and T_4 (b); T_5 and T_6 (c); T_7 and T_8 (d); ϕ_1 and ϕ_2 (e).

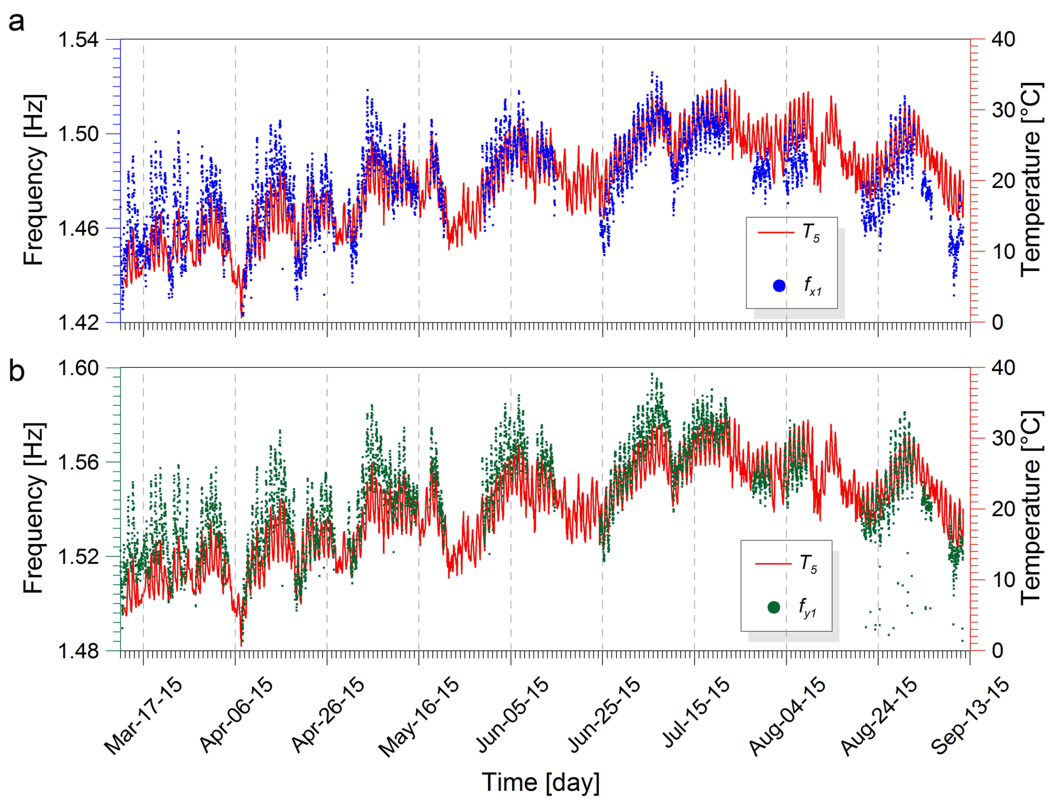

Figure 6: Correlation between frequencies and temperature data: f_{x1} and T_5 (a); f_{y1} and T_5 (b).

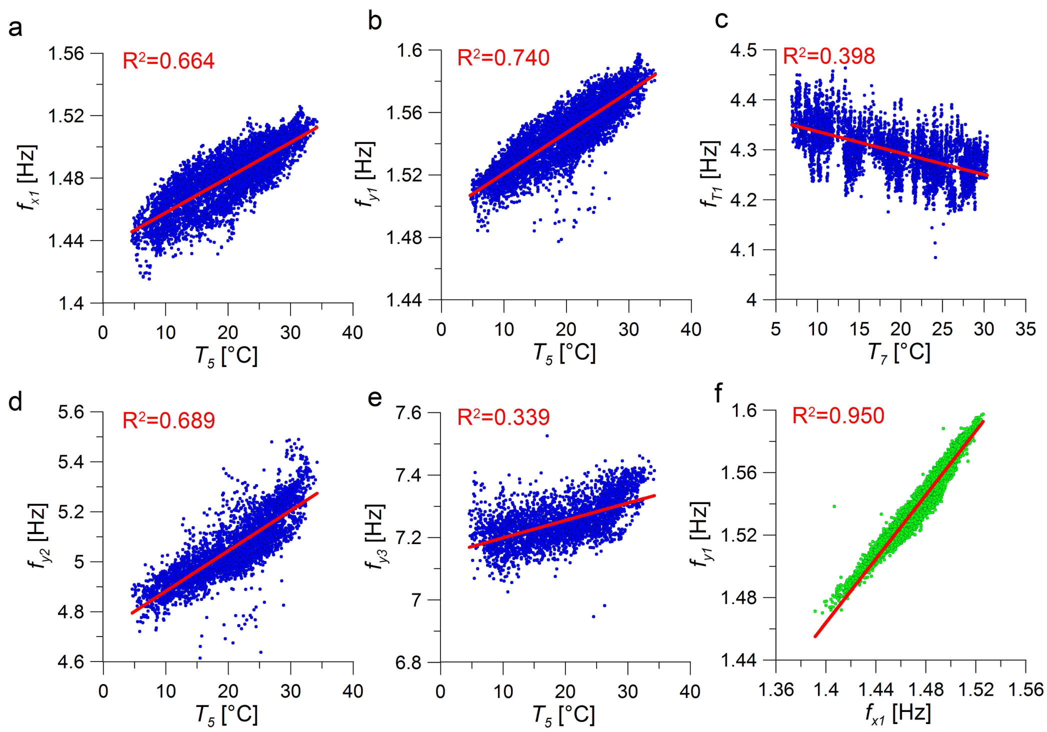

Figure 7: Correlation between frequencies and temperature data (a-e) and resulting correlation between natural frequencies of modes Fx1 and Fy1.

	T_1	T_2	T_3	T_4	T_5	T_6	T_7	T_8	ϕ_1	ϕ_2
T_1	1.00	0.77	0.99	0.98	0.95	0.94	0.99	0.99	-0.40	-0.34
T_2		1.00	0.80	0.82	0.89	0.90	0.71	0.72	-0.33	-0.58
T_3			1.00	1.00	0.97	0.96	0.97	0.97	-0.35	-0.37
T_4				1.00	0.98	0.97	0.96	0.97	-0.34	-0.38
T_5					1.00	0.99	0.91	0.91	-0.32	-0.46
T_6						1.00	0.90	0.91	-0.34	-0.48
T_7							1.00	1.00	-0.39	-0.30
T_8								1.00	-0.38	-0.30
ϕ_1									1.00	0.56
ϕ_2										1.00

Table 3: Correlation coefficients between environmental parameters.

	f_{x1}	f_{y1}	f_{T1}	f_{y2}	f_{y3}
f_{x1}	1.00	0.97	-0.15	0.85	0.31
f_{x2}		1.00	-0.24	0.90	0.29
f_{T1}			1.00	-0.29	0.56
f_{y2}				1.00	0.32
f_{y3}					1.00

Table 4: Correlation coefficients between frequencies.

temperature data collected in different positions of the bell tower. In fact, the construction geometry, affecting the periodical differential solar shading of the masonry parts and the variable materials and walls' thickness motivate the local thermal investigation carried out in this work. Just as an example, the outdoor temperature T_2 is the one showing the lowest correlation coefficients with other temperature data, showing that the peculiar and local construction characteristics affect the differential thermal behavior of such a complex case study building that should not be neglected in SHM analysis. A significant difference between indoor and outdoor surface temperatures is observed owing to the large width of the masonry, which is apparent by looking at the relatively low correlation between T_2 and T_3. Indoor surface and air temperatures within the shaft of the tower are very well correlated and numerically similar, regardless of the orientation of the sensors, which is apparent by inspecting the correlation between T_3 and T_4. The orientation becomes slightly more important in the case of temperature sensors located outdoor, due to the effect of solar radiation. Although the correlation between T_5 and T_6 is very high, differences in peak values are visible in Figure

	T_1	T_2	T_3	T_4	T_5	T_6	T_7	T_8	ϕ_1	ϕ_2
f_{x1}	0.67	0.76	0.75	0.76	0.82	0.80	0.59	0.60	-0.12	-0.39
f_{y1}	0.73	0.78	0.81	0.82	0.86	0.85	0.67	0.68	-0.15	-0.39
f_{T1}	-0.57	-0.22	-0.50	-0.48	-0.41	-0.41	-0.63	-0.62	0.18	0.00
f_{y2}	0.76	0.75	0.81	0.82	0.83	0.83	0.71	0.72	-0.35	-0.47
f_{y3}	0.53	0.54	0.57	0.57	0.58	0.58	0.49	0.50	-0.35	-0.32

Table 5: Correlation coefficients between frequencies and environmental parameters.

5. One last observation concerns air temperature within the cusp, which is seen to undergo very small daily fluctuations conceivably because of the high transmittance and low thermal capacity of the roof of the tower.

Correlation coefficients between temperature data and air humidity are remarkably low and negative in sign, due to a decrease in relative air humidity with increasing air temperature.

Correlation coefficients between natural frequencies are summarized in Table 4. These results generally show a high degree of correlation between the natural frequencies of modes Fx1, Fy1 and Fy2. The torsional mode, T1 exhibits a significant correlation only with mode Fy3 that, in turn, is only slightly correlated with other modes.

The reason for the high degree of statistical correlation between natural frequencies is imputable to their dependency on environmental parameters. Table 5 summarizes such correlations highlighting, in particular, that all frequencies, with the exception of f_{T1}, exhibit positive correlation coefficients with temperature profiles, indicating therefore an increase in natural frequency with increasing temperature, in agreement with other literature works and conceivably attributable to closing of micro-cracks within mortar layers due to thermal expansion [6, 7]. The negative correlations between f_{T1} and temperature data is worth noting and it is here attributed to the thermally-induced slackening of tie elements and of fiber reinforcements installed during the retrofit of 2002 (cfr. Section 2.1), reducing the lateral confinement and thus determining a softening effect on the dynamic behavior of the tower. Another remark on the results is that, with the exception of mode $T1$, temperature T_5 is the environmental parameter that corresponds to the largest correlations with natural frequencies. It is, therefore, placed in the best location for an effective removal of environmental effects from natural frequencies.

Figure 6 shows superimposed time history plots of natural frequencies and

f_i	T_{s_i}	$f_{i,0}$ (Hz)	$\kappa_{i,T}$ (mHz/°C)
f_{x1}	T_5	1.435	2.25
f_{y1}	T_5	1.495	2.61
f_{T1}	T_7	4.380	-4.31
f_{y2}	T_5	4.721	16.17
f_{y3}	T_5	7.143	5.58

Table 6: Parameters of best fitting lines between frequencies and temperature data.

temperature data, considering the frequencies of the first two bending modes and temperature data T_5. These plots visually emphasize the frequency-temperature correlations, showing in particular that daily fluctuations of natural frequencies are determined by daily fluctuations of temperature and that long-term increments of natural frequencies during the monitoring period are determined by seasonal increments in temperature.

Figure 7 shows plots of natural frequencies against the temperature data for which they exhibit the maximum absolute values of the correlation coefficients. These plots show that frequency-temperature correlations are almost linear, as confirmed by the relatively high values of the coefficient of determination, R^2, obtained through best fitting linear trends. The best fitting lines in Figure 7 have the following general equation:

$$f_i = f_{i,0} + \kappa_{i,T} T_{s_i} \tag{5}$$

where $i = x_1, x_2, T, y_2, y_3$ indicates the mode, s_i is the number of the temperature sensor corresponding the largest absolute correlation coefficient with f_i, while $f_{i,0}$ and $\kappa_{i,T}$ are frequency at 0 ℃ and frequency-temperature sensitivity coefficients, respectively, whose least square estimates are summarized in Table 6. The relatively high values of $\kappa_{i,T}$ demonstrate the significant variations of natural frequencies with temperature. In particular, it should be noticed that, according to the results reported in Table 6, a temperature change of 10 ℃ produces relative changes in natural frequencies between 0.8 and 3.4%, which can be considered as large in comparison with changes in natural frequencies typically produced by small damages in full-scale structures [22].

Correlations between frequencies and relative humidity data, in Table 5, also deserve some attention. In particular, the negative correlations between natural frequencies and humidities, with the only exception of mode $T1$, could be interpreted in light of the negative correlations between humidity and temperature, as well as to a slight mass increment due to moisture in the masonry. However, correlations observed in this work are too weak to reliably conclude about the physical mechanisms governing humidity effects on natural frequencies.

3.3. Freezing conditions

Sudden increases in natural frequencies of the bell tower were observed during the earliest days of 2015. This happened before implementing the environmental monitoring hardware described in Section 2.2. In order to properly interpret this behavior, frequencies identified during those days have been inspected in relation to temperature data recorded from a nearby weather monitoring station located in the historical center of Perugia. Results are shown in Figure 8 and clearly demonstrate that the increases in natural frequencies occurred during three consecutive freezing days, in which temperature was steadily below 0 ℃. In particular, natural frequencies increased in time for the whole freezing period, while started to decrease and to recover the original values right after temperature raised over 0 ℃.

The results showed in Figure 8, although not permitting a significant statistical analysis, clearly demonstrate that frequency-temperature correlations drastically change in freezing conditions. Contrarily to what observed in above 0 ℃ conditions, frequencies below 0 ℃ increase with decreasing temperature. This circumstance is conceivably caused by the stiffening effect produced by ice forming within the micro-pores of the masonry. Resulting variations in natural frequencies seem to be progressively more significant in higher order modes, which might be related to faster freezing of the belfry with respect to the shaft. The case of the third bending mode in the y direction, mode Fy3, is especially noteworthy in Figure 8: its frequency, in a continuously freezing time period of about three days, exhibited a remarkable increase of about 20%, that roughly corresponds to a 40% increase in structural stiffness.

4. Statistical reconstruction of natural frequencies

4.1. Effect of training data on prediction errors

As discussed in Section 2.4, natural frequencies can be independently estimated using environmental parameters as predictors of MLR models, Eq. (2). The use of linear statistical models is in this case supported by the

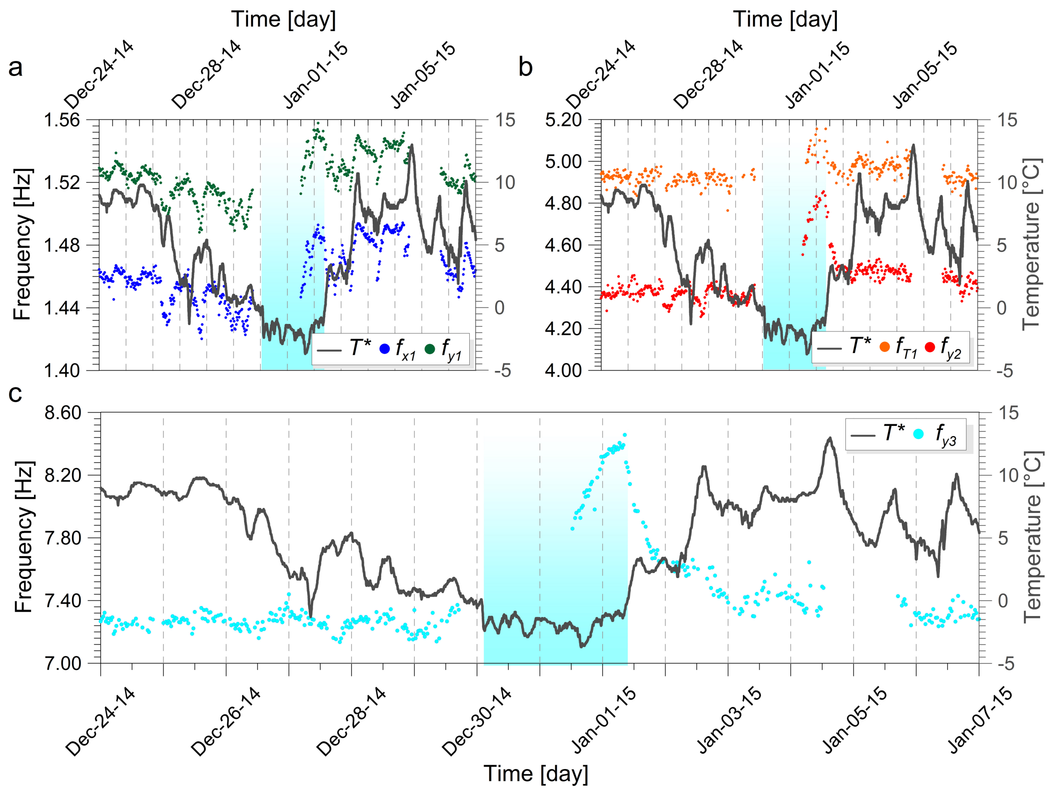

Figure 8: Time history plots of identified natural frequencies and temperature data between December 24th 2014 and January 8th 2015 (the area in blue indicates the period with temperature below 0 C): time histories of f_{x1} and f_{y1} (a); time histories of f_{T1} and f_{y2} (b); time history of f_{y3} (c).

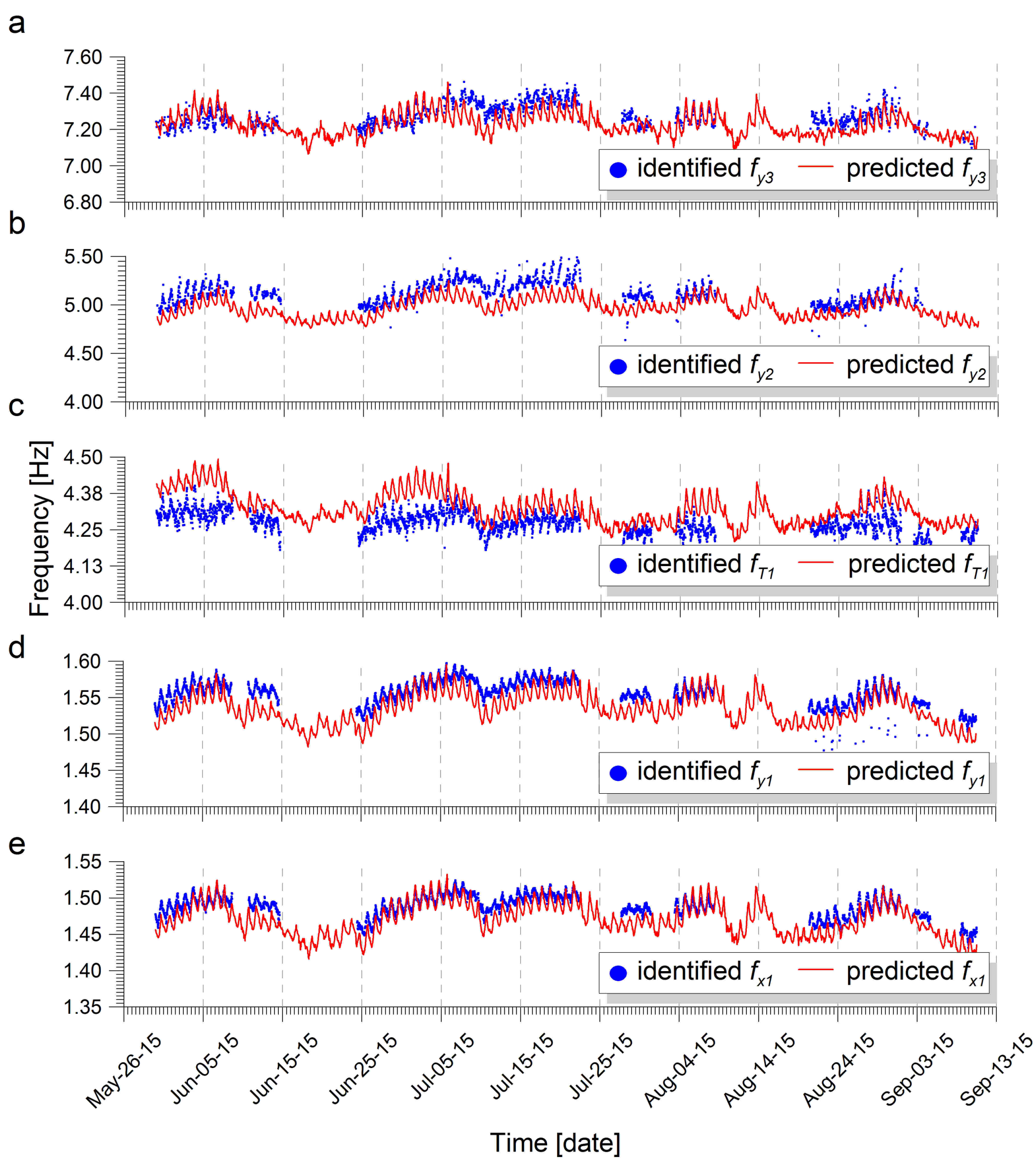

Figure 9: Identified and statistically predicted natural frequencies.

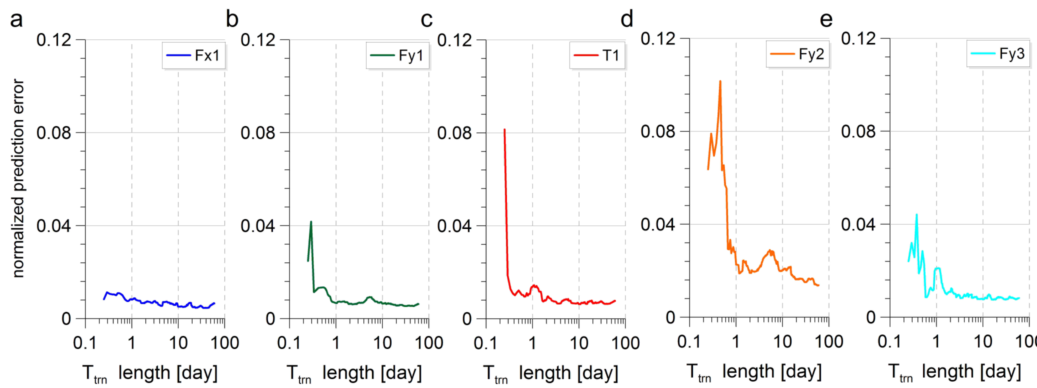

Figure 10: Normalized prediction error of MLR model versus training period length: mode Fx1 (a); mode Fy1 (b); mode T (c); mode Fy2 (d); mode Fy3 (e).

observed linearity of the correlations between natural frequencies and temperature data.

In order to obtain accurate frequency predictions, it is necessary to estimate the coefficients of MLR models using data recorded in a sufficiently long training period. As an example, Figure 9 shows identified and predicted frequencies in the observation period, using a training period of sixty days and using all available environmental monitoring sensors. The good quality of the statistical reconstruction of the frequencies is apparent, especially for low order modes.

The effect of a change in the length of the training period on the prediction error of the statistical model is investigated in Figure 10. For each mode, the error is computed as the root mean square of the difference between identified and predicted natural frequency values, normalized by the variance of the identified natural frequency values. The error is computed in the same observation period of 65 days following the longest training period of 60 days. The results show that statistical models' accuracy stabilizes very quickly after about 10 days. The residual error after proper training represents the part of variance in identified frequencies that is not related to environmental effects, while it is essentially determined by random errors in output only modal identification.

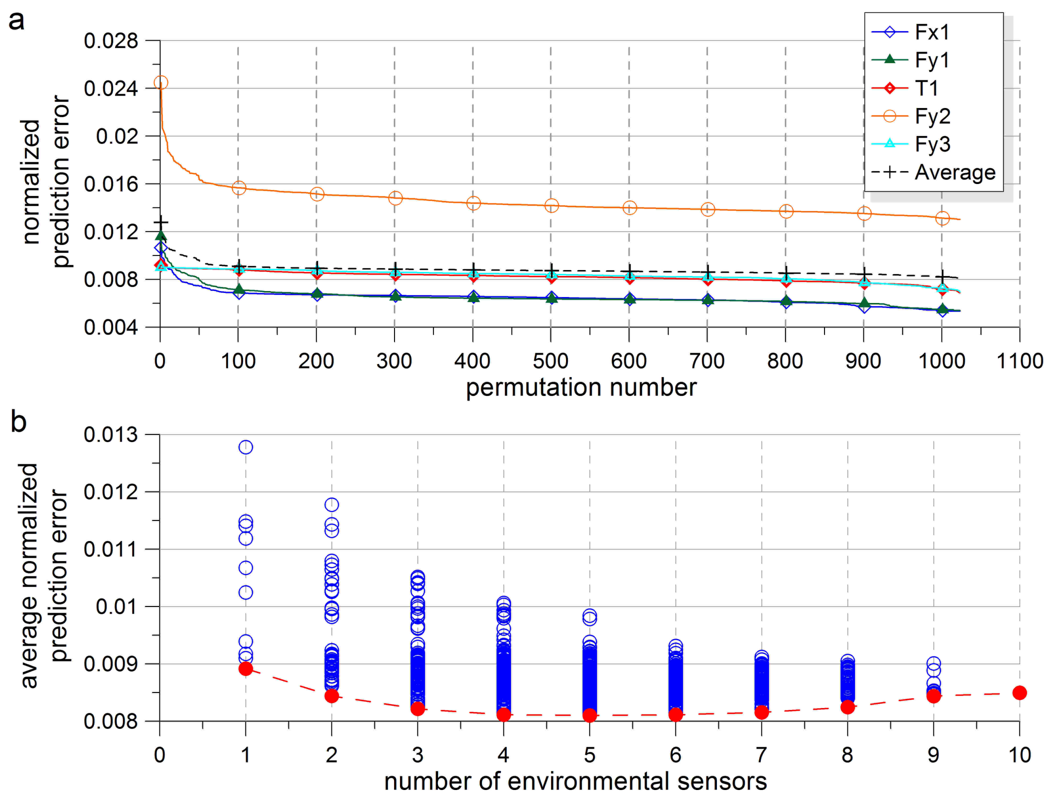

Figure 11: Prediction accuracy with all possible permutations of environmental monitoring sensors: prediction errors sorted in descending order (a); average normalized prediction error versus number of sensors (b).

No. of sensors	Error	Optimal layout
1	8.917e-3	$[T_5]$
2	8.439e-3	$[T_1 \quad T_4]$
3	8.214e-3	$[T_5 \quad T_7 \quad T_8]$
4	8.111e-3	$[T_1 \quad T_4 \quad T_5 \quad \phi_1]$
5	8.100e-3	$[T_1 \quad T_3 \quad T_4 \quad T_5 \quad \phi_1]$
6	8.110e-3	$[T_1 \quad T_3 \quad T_4 \quad T_5 \quad T_6 \quad \phi_1]$
7	8.154e-3	$[T_1 \quad T_3 \quad T_4 \quad T_5 \quad T_6 \quad \phi_1 \quad \phi_2]$
8	8.244e-3	$[T_1 \quad T_2 \quad T_3 \quad T_4 \quad T_5 \quad T_6 \quad \phi_1 \quad \phi_2]$
9	8.437e-3	$[T_1 \quad T_3 \quad T_4 \quad T_5 \quad T_6 \quad T_7 \quad T_8 \quad \phi_1 \quad \phi_2]$
10	8.492e-3	$[T_1 \quad T_2 \quad T_3 \quad T_4 \quad T_5 \quad T_6 \quad T_7 \quad T_8 \quad \phi_1 \quad \phi_2]$

Table 7: Optimal environmental sensors' layouts for natural frequency prediction.

4.2. Optimal layout of hygrothermal monitoring sensors

A major aspect to be considered in practical applications is limiting the number of monitoring sensors of ambient relative humidity, dry bulb and masonry superficial temperature to what strictly necessary to achieve good frequency estimates. In order to investigate this aspect for the considered case study, Figure 11 shows the evolution of normalized prediction errors in all of the 1023 possible sensors' layouts using some or all of the 10 environmental sensors considered in this paper. The error is computed as in the case of Figure 10 and the average error is computed by considering all five continuously identified modes. The optimal sensors layouts for varying number of sensors are summarized in Table 7.

The presented results show that one single optimally located sensor can be sufficient to achieve about 90% of the accuracy that can be achieved with more than one sensor. In the present case, the optimal sensor is T_5 as it is the one exhibiting the largest correlations with natural frequencies. By increasing the number of predictors, the accuracy improves if the sensors' are deployed in different locations along the tower, in such a way to consider different portions of the structure and different exposures to environmental forcing. In general, air temperature sensors seem to be more informative than surface temperature sensors and the best statistical prediction accuracy is achieved with five sensors, while further enlarging the number of sensors can be even detrimental. Humidity starts to play a significant role if coupled with at least three temperature sensors but it is necessary to attain the best prediction accuracy.

5. Conclusions

The paper has investigated the effects of changes in environmental conditions on the natural frequencies of a continuously monitored monumental masonry bell tower. The topic is relevant for vibration-based structural health monitoring using natural frequencies as damage sensitive features.

The results have shown that dry bulb temperature variations can produce significant changes in natural frequencies, up to 16 mHz/°C, while effects of air humidity are relatively marginal.

Three temperature-driven types of frequency variation phenomena have been observed. The first one is the increase in the eigenfrequencies of bending modes with increasing temperature, due to thermal expansion in the masonry determining closing of micro-cracks in mortar layers, which was already observed in other literature works. The second one is the decrease of torsional eigenfrequencies with increasing temperature, which is attributed to thermally-induced slackening of tie elements and of fiber reinforcements. The third one is the increase in natural frequencies with decreasing temperature which occurs in freezing conditions due to ice forming within the micro-pores of the masonry.

When continuously identified natural frequencies are used for structural health assessment purposes, temperature effects need to be carefully removed. Results presented in this paper show that multivariate linear regressions are effective for this purpose, as statistical correlations between frequencies and temperature are remarkably linear.

The optimal statistical reconstruction of natural frequencies of the monitored tower required the use of four temperature sensors (air and surface thermal measurements) and one humidity sensor, located at different heights and in different regions of the tower characterized by similar material and geometrical characteristics but different environmental exposure to solar radiation, winds, etc. However, one optimally located air temperature sensor with a Southward exposure was found sufficient to achieve about 90% of the statistical prediction accuracy that was achieved with more than one sensor. In general, the accuracy of such reconstruction increases with the length of the training period, but a very fast convergence was evidenced, which indicated that about 10 days of training period were already sufficient to gain relatively accurate predictions.

6. Acknowledgments

The Authors gratefully acknowledge the financial support of the “Cassa di Risparmio di Perugia” Foundation that funded this study through the project ”Structural Monitoring for the protection of the Cultural Heritage: the bell tower of the Basilica of San Pietro in Perugia and the dome of the Basilica of Santa Maria degli Angeli in Assisi” (Project Code 2014.0266.021). The environmental monitoring are carried out thanks to the support of the same “Cassa di Risparmio di Perugia” Foundation that supported the project entitled ”UMBRA ARTIS: Energy technologies for monitoring and protecting artworks in subterranean environment” (Project Code 2014.0223.021).

The authors also wish to gratefully thank the “Fondazione per l’Istruzione Agraria” in Perugia, for granting access to the tower and for technical and logistic support, as well as Arch. Francesco Ventura, for providing precious information on the bell tower, including architectural survey data.

The fourth author acknowledgments are due to the “CIRIAF program for UNESCO” in the framework of the UNESCO Chair “Water Resources Management and Culture”, for supporting her research.

References

[1] A. Deraemaeker, R. E., G. De Roeck, J. Kullaa, Vibration-based structural health monitoring using output-only measurements under changing environment, Mech Syst Signal Proc 22 (2008) 34 – 56.

[2] A. Alvandi, C. Cremona, Assessment of vibration-based damage identification techniques, J Sound Vib 292 (2006) 179–202.

[3] A. L. Materazzi, F. Ubertini, Eigenproperties of suspension bridges with damage, Journal of Sound and Vibration 330 (2011) 6420 – 6434.

[4] C. Farrar, K. Worden, An introduction to structural health monitoring, Phil. Trans. R. Soc. As. 365 (2007) 303–315.

[5] J. Ko, Y. Ni, Technology developments in structural health monitoring of large-scale bridges, Engineering Structures 27 (2005) 1715 – 1725.

[6] L. Ramos, L. Marques, P. Lourenco, G. De Roeck, A. Campos-Costa, J. Roque, Monitoring historical masonry structures with operational

modal analysis: Two case studies, Mechanical Systems and Signal Processing 24 (2010) 1291–1305.

[7] A. Saisi, C. Gentile, M. Guidobaldi, Post-earthquake continuous dynamic monitoring of the gabbia tower in mantua, italy, Constr Build Mater 81 (2015) 101 – 112.

[8] C. A. Calcada, M., R. Delgado, Dynamic analysis of metallic arch railway bridge, J Bridge Eng 7 (2002) 214–222.

[9] C. Spyrakos, I. Raftoyiannis, J. Ermopoulos, Condition assessment and retrofit of a historic steel-truss railway bridge, J Constr Steel Res 60 (2004) 1213–1225.

[10] A. Brencich, D. Sabia, Experimental identification of a multi-span masonry bridge: the tanaro bridge, Constr Build Mater 22 (2008) 2087–2099.

[11] B. Jaishi, W. Ren, Z. Zong, P. Maskey, Dynamic and seismic performance of old multi-tiered temples in nepal, Eng Struct 25 (2003) 1829–1839.

[12] F. Casarin, C. Modena, Seismic assessment of complex historical buildings: Application to reggio emilia cathedral, italy, Int J Archit Herit 2 (2008) 304–327.

[13] A. Pau, F. Vestroni, Vibration analysis and dynamic characterization of the colosseum, Struct Control Health Monit 15 (2008) 1105–1121.

[14] F. Aras, L. Krstevska, G. Altay, L. Tashkov, Experimental and numerical modal analyses of a historical masonry palace, Constr Build Mater 25 (2011) 81–91.

[15] S. Bennati, L. Nardini, W. Salvatore, Dynamic behaviour of a medieval masonry bell tower. ii. measurement and modelling of the tower motion, J Struct Eng 131 (2005) 1656–1664.

[16] S. Ivorra, F. J. Pallar Dynamic investigations on a masonry bell tower, Eng Struct 28 (2006) 660 – 667.

[17] C. Gentile, A. Saisi, Ambient vibration testing of historic masonry towers for structural identification and damage assessment, Constr Build Mater 21 (2007) 1311–1321.

[18] F. PeauthorP. B. Lourenco, N. Mendes, D. V. Oliveira, Numerical models for the seismic assessment of an old masonry tower, Eng Struct 32 (2010) 1466 – 1478.

[19] C. S. Oliveira, E. Cakti, D. Stengel, M. Branco, Minaret behavior under earthquake loading: The case of historical istanbul, Earthq Eng Struct Dyn 41 (2012) 19–39.

[20] D. Foti, M. Diaferio, N. Giannoccaro, M. Mongelli, Ambient vibration testing, dynamic identification and model updating of a historic tower, NDT E Int 47 (2012) 88–95.

[21] C. Gentile, A. Saisi, A. Cabboi, Structural identification of a masonry tower based on operational modal analysis, Int J Archit Herit 9 (2015) 98–110.

[22] F. Magalh, A. Cunha, E. Caetano, Vibration based structural health monitoring of an arch bridge: From automated oma to damage detection, Mech Syst Signal Proc 28 (2012) 212 – 228.

[23] F. Magalh, A. Cunha, E. Caetano, Online automatic identification of the modal parameters of a long span arch bridge, Mech Syst Signal Proc 23 (2009) 316 – 329.

[24] C. Rainieri, G. Fabbrocino, Automated output-only dynamic identification of civil engineering structures, Mech Syst Signal Proc 24 (2010) 678 – 695.

[25] F. Ubertini, C. Gentile, A. Materazzi, Automated modal identification in operational conditions and its application to bridges, Eng Struct 46 (2013) 264–278.

[26] L. Hui, S. Li, J. Ou, H. Li, Modal identification of bridges under varying environmental conditions: Temperature and wind effects, Struct. Control Health Monit. 17 (2010) 495–512.

[27] K. Worden, H. Sohn, C. Farrar, Novelty detection in a changing environment: regression and interpolation approaches, J Sound Vib 258 (2002) 741 – 761.

[28] A. Yan, G. Kerschen, P. De Boe, J. Golinval, Structural damage diagnosis under varying environmental conditions part i: a linear analysis, Mech Syst Signal Proc 19 (2005) 847 – 864.

[29] A. Yan, G. Kerschen, P. De Boe, J. Golinval, Structural damage diagnosis under varying environmental conditions part ii: local pca for non-linear cases, Mech Syst Signal Proc 19 (2005) 865 – 880.

[30] A. Bellino, A. Fasana, L. Garibaldi, S. Marchesiello, Pca-based detection of damage in time-varying systems, Mech Syst Signal Proc 24 (2010) 2250–2260.

[31] A. Mosavi, D. Dickey, R. Seracino, S. Rizkalla, Identifying damage locations under ambient vibrations utilizing vector autoregressive models and mahalanobis distances, Mech Syst Signal Proc 26 (2012) 254 – 267.

[32] G. Comanducci, F. Ubertini, A. Materazzi, Structural health monitoring of suspension bridges with features affected by changing wind speed, J Wind Eng Ind Aerodyn 141 (2015) 12–26.

[33] R. Vetturini, Campanile del complesso monumentale di san pietro in perugia (in italian), document available online at http://divisare.com/projects/247982-riccardo-vetturini-campanile-del-complesso-monumentale-di-s-pietro-in-perugia, 2014.

[34] I. The MathWorks, MATLAB R2012a, Natick, Massachusetts, United States, 2012.

[35] A. L. Pisello, C. Piselli, F. Cotana, Thermal-physics and energy performance of an innovative green roof system: The cool-green roof, Solar Energy 116 (2015) 337 – 356.

[36] A. L. Pisello, A. Petrozzi, V. L. Castaldo, F. Cotana, On an innovative integrated technique for energy refurbishment of historical buildings: Thermal-energy, economic and environmental analysis of a case study, Applied Energy (2015).

[37] A. L. Pisello, G. Pignatta, V. L. Castaldo, F. Cotana, The impact of local microclimate boundary conditions on building energy performance, Sustainability 7 (2015) 9207–9230.

[38] R. Cantieni, Experimental methods used in system identification of civil engineering structures, in: International Operational Modal Analysis Conference (IOMAC 05).

[39] V. Overschee, D. Moor, Subspace Identification for Linear Systems: Theory - Implementation - Applications, Kluwer Academic Publishers, 1996.